



LOFT

Overview of the Strong Gravity Working Group

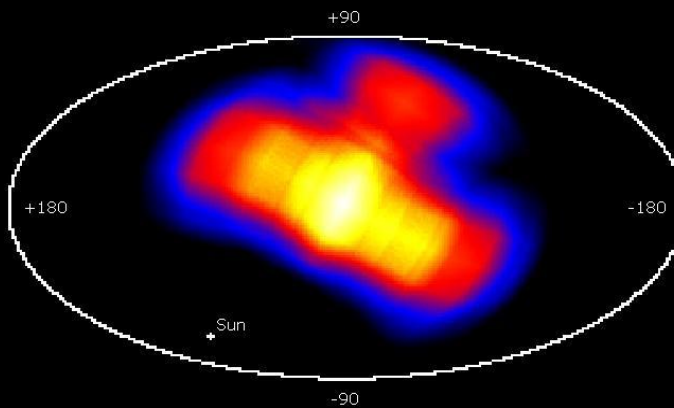
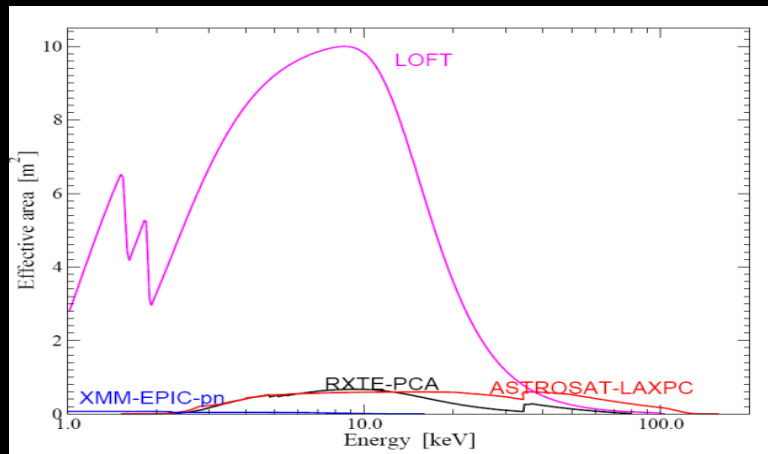
Luigi Stella

on behalf of the LOFT Consortium

The LOFT "Strong Gravity" Science Group

- D. Barret* (IRAP, France)
D. Altamirano (Univ. of Amsterdam, Netherlands)
P. Bakala (Silesian University, Czech Republic)
T. Belloni (INAF-OAB, Italy)
L. Burderi (Cagliari University, Italy)
M. Bursa (Prague Astron. Institute, Czech Republic)
E. Cackett (Wayne State University , United States)
S. Campana (INAF-OA Brera, Italy)
D. Lin (IRAP, France)
A. De Rosa (IASF/INAF Rome, Italy)
T. di Salvo (Univ. of Palermo, Italy)
A. Fabian (Cambridge University, UK)
M. Gilfanov (MPA Garching, Germany)
K. Goluchová (Silesian University, Czech Republic)
A. R. Ingram (Univ. of Amsterdam, NL)
T. Johannsen (Perimeter Inst. for Theor. Physics, Canada)
P. Jonker (SRON, The Netherlands)
P. Kaaret (University of Iowa, United States)
V. Karas (Prague Astron. Institute, Czech Republic)
M. van der Klis (University of Amsterdam, The Netherlands)
W. Klužniak (Copernicus Astronomical Center, Poland)
- D. Lai (Cornell University, USA)
F. K. Lamb (University of Illinois, USA)
G. Lodato (Universita degli Studi di Milano, Italy)
G. Matt (Univ. of Rome 3, Italy)
S. Migliari (Univ. of Barcelona, Spain)
C. Miller (University of Maryland, United States)
G. Miniutti (CSIC/INTA, Spain)
S. Motta (INAF-OAB, Italy)
N. Nowak (MIT, United States)
A. Patruno (University of Amsterdam, The Netherlands)
J. Poutanen (University of Oulu, Finland)
C. Reynolds (University of Maryland, United States)
L. Rezzolla (MPI for Gravitational Physics, Germany)
G. Torok (Silesian University, Czech Republic)
A. Sanna (Univ. of Groningen, The Netherlands)
J. Schee (Silesian University, Czech Republic)
L. Stella (INAF-OAR, Italy)
Z. Stuchlik (Silesian University, Czech Republic)
P. Utthley (University of Amsterdam, The Netherlands)
P. Varniere (APC, France)
S. Vaughan (Leicester University , United Kingdom)
S. Watanabe (ISAS, Japan)

LOFT Instruments



LAD – Large Area Detector

Effective Area	4 m ² @ 2 keV 8 m ² @ 5 keV 10 m ² @ 8 keV 1 m ² @ 30 keV
Energy range	2-30 keV primary 30-80 keV extended
Energy resolution FWHM	260 eV @ 6 keV 200 eV @ 6 keV (45% of area)
Collimated FoV	1 degree FWHM
Time Resolution	10 µs
Absolute time accuracy	1 µs
Dead Time	<1% at 1 Crab
Background	<10 mCrab (<1% syst)
Max Flux	500 mCrab full event info 15 Crab binned mode

WFM- Wide Field Monitor

Energy range	2-50 keV primary 50-80 keV extended
Active Detector Area	1820 cm ²
Energy resolution	300 eV FWHM @ 6 keV
FOV (Zero Response)	180°x90° + 90°x90°
Angular Resolution	5' x 5'
Point Source Location Accuracy (10- σ)	1' x 1'
Sensitivity (5- σ , on-axis)	Galactic Center, 3 s Galactic Center, 1 day
	270 mCrab 2.1 mCrab
Standard Mode	5-min, energy resolved images
Trigger Mode	Event-by-Event (10µs res) Realtime downlink of transient coordinates

LOFT and ESA's Cosmic Vision program

3.3 Matter under extreme conditions

Probe gravity theory in the very strong field environment of black holes and other compact objects, and the state of matter at supra-nuclear energies in neutron stars

- ⌚ Does matter orbiting close to a Black Hole event horizon follow the predictions of General Relativity?



Strong Gravity

Strong Gravity

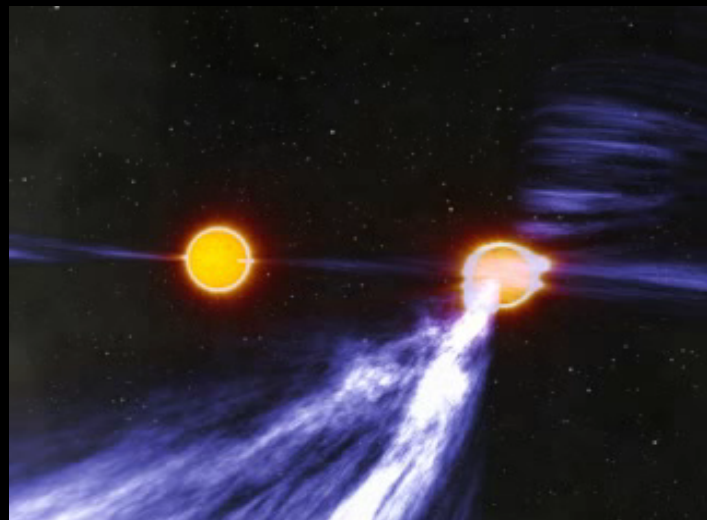
Relativistic Binary pulsars with at least 1 post-newtonian parameter measured

- periastron advance,
- orbital decay,
- time-dilation and gravitational red-shift parameter,
- sin of the inclination of the orbit (equal, in GR, to the shape parameter of the Shapiro delay)
- mass of the companion star (equal, in GR, to the range parameter of the Shapiro delay)

* Accurate test of gravity; several GR effects confirmed with very good accuracy

(Possenti Burgay 2011)

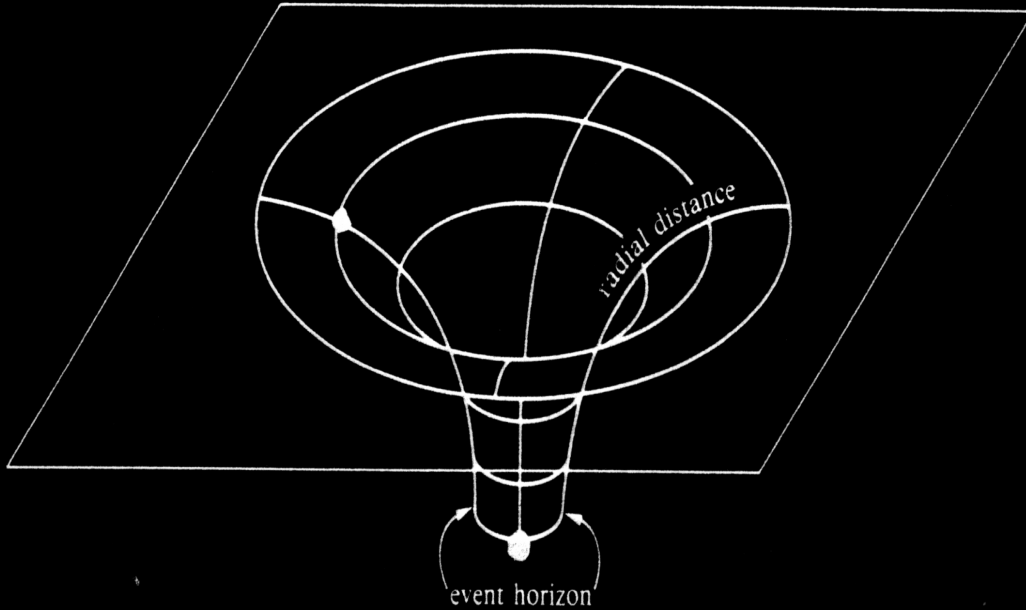
* BUT: direct measurements only at large radii
($R \sim 10^6$ Schwarzschild radii)



J0024-7204H*
J0024-7204J*
J0045-7319
J0437-4715**
J0514-4002A*
J0621+1002
J0737-3039A
J0737-3039B
J0751+1807
J0823+0159
J1022+1001
J1023+0038**
J1141-6545
J1518+4904**
J1537+1155
J1600-3053
J1603-7202
J1614-2230
J1623-2631*,**
J1640+2224
J1713+0747
J1740-3052
J1748-2021B*
J1750-3703A*
J1750-3703B*
J1756-2251
J1802-2124
J1804-0735*
J1811-1736
J1823-1115
J1829+2456
J1857+0943
J1903+0327
J1906+0746
J1909-3744**
J1915+1606
J1959+2048**
J2019+2425
J2051-0827
J2129+1210C
J2145-0750**
J2305+4707

Strong Field Effects

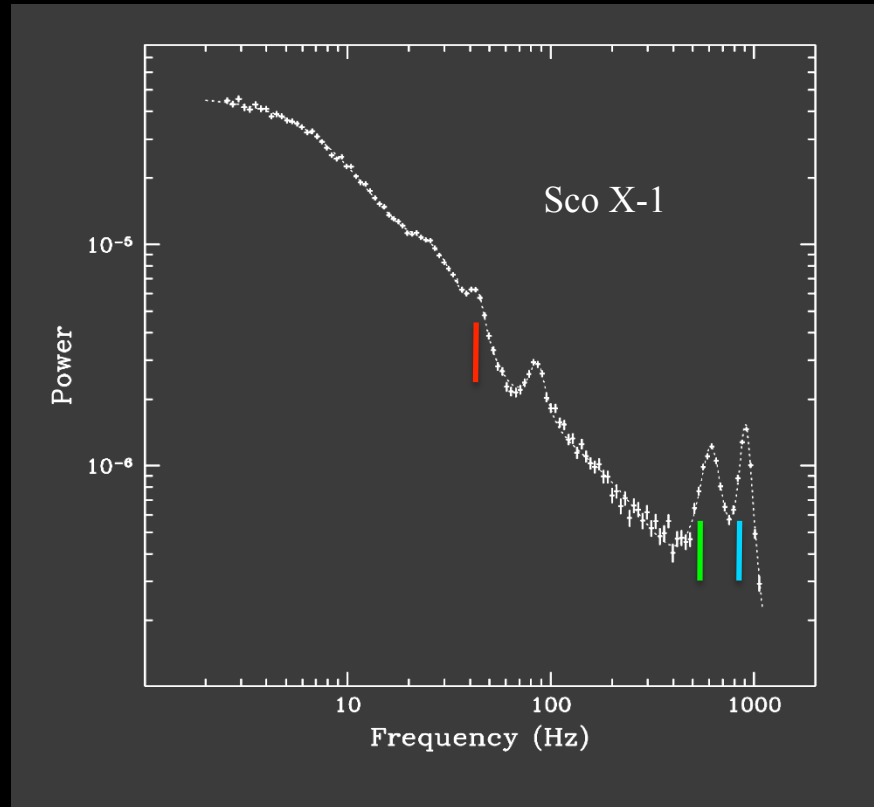
Need to sample Radii close to the horizon ($R_g \sim GM/c^2$): matter accretion into black holes and neutron stars provides the best tool.



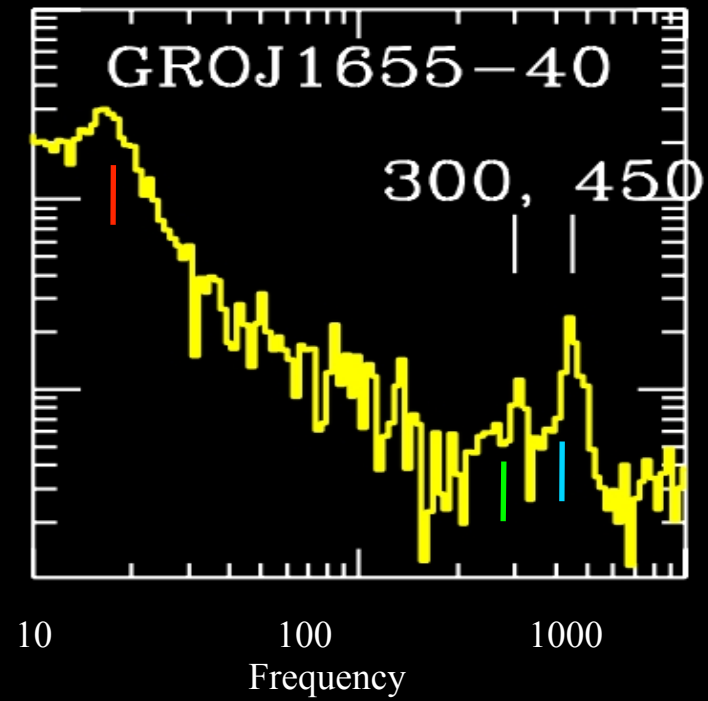
- Last Stable Circular orbit, aka ISCO ($6 R_g \rightarrow 1 R_g$)
- Particle motion around ISCO and fundamental frequencies of motion
- Dragging of inertial frame
- Strong field light deflection
- Black hole mass and spin

Strong Field Diagnostic: Quasi Periodic Oscillations

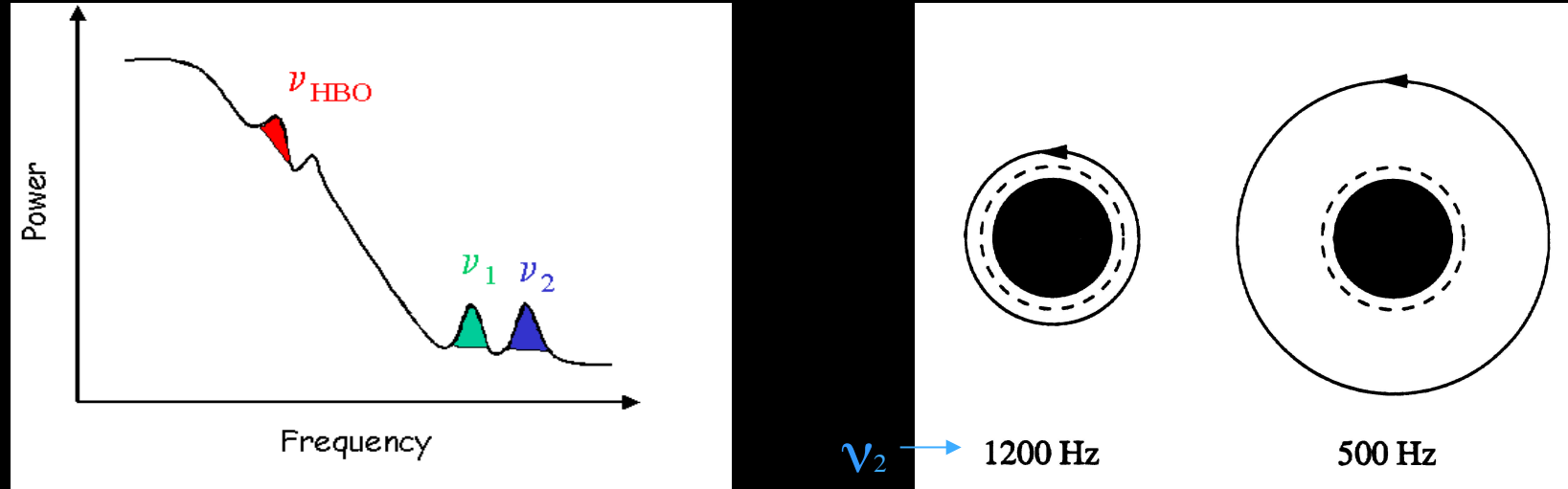
Accreting neutron stars



Accreting black hole candidates



Generic Model for higher frequency kHz QPOs



A 10 km radius, $1.4 M_{\odot}$ neutron star with the corresponding innermost circular stable orbit (ISCO; dashed circle) and orbits (drawn circles) corresponding to orbital frequencies of 1200 and 500 Hz, drawn to scale.

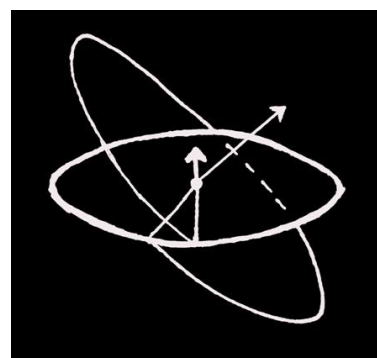
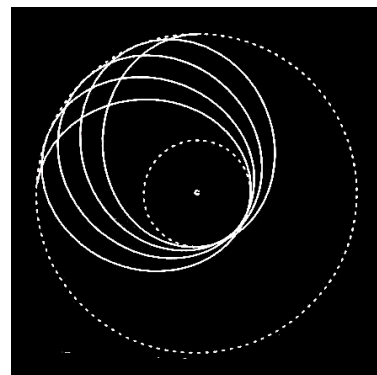
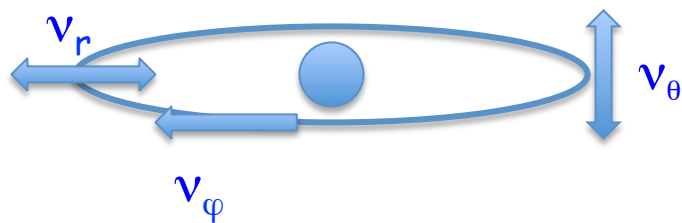
$\nu_2 = \nu_{\varphi}(r_i)$ = Keplerian (φ) frequency at inner disk radius r_i

$$r_i \approx 15 (M/M_{\odot}) (\nu_2 / 1000 \text{ Hz})^{-2/3} \text{ km}$$

$r_i = f(\dot{M})$ to explain frequency variations

(Alpar, Shaham 1985;
Strohmayer et al. 1996;
Lamb et al. 1985;
Miller et al. 1997)

Fundamental Frequencies of Particle Motion

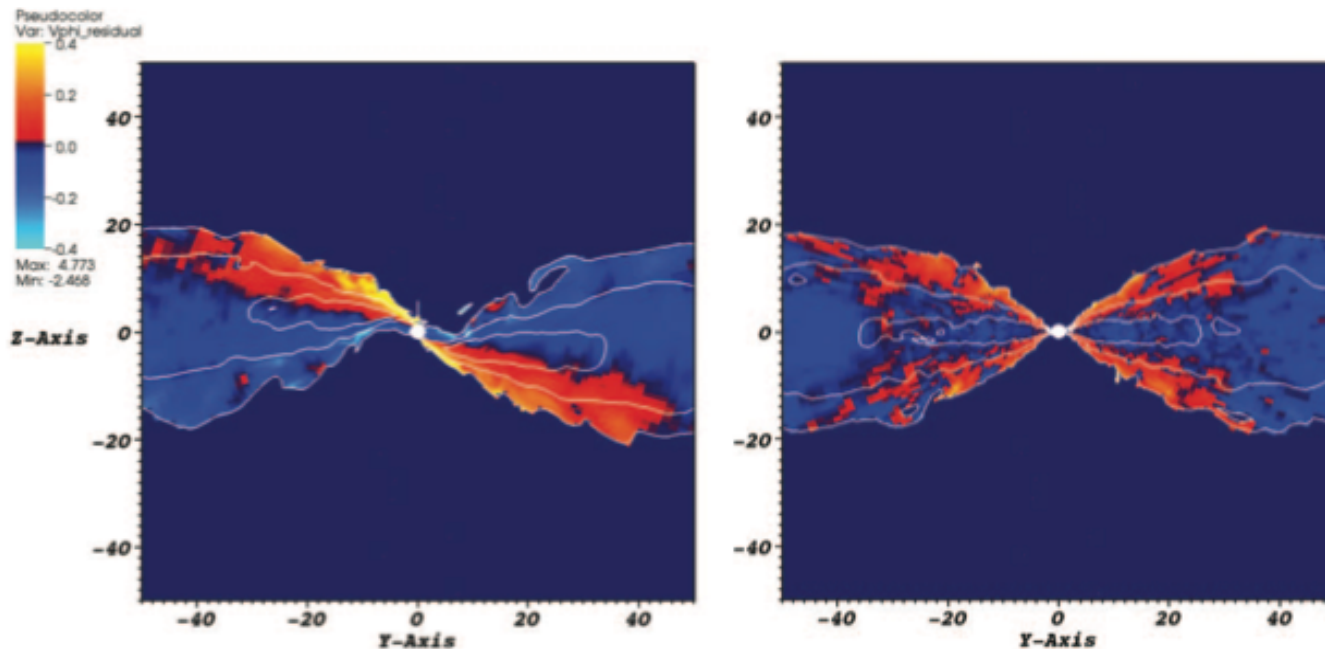


- Epicyclic Resonance (fixed radii)

- Relativistic Precession: nodal and periastron (variable radius)

Accretion Disk - Numerical Simulations

- No clear QPO signals yet
- Epicyclic frequencies play a role in some tilted disk simulations

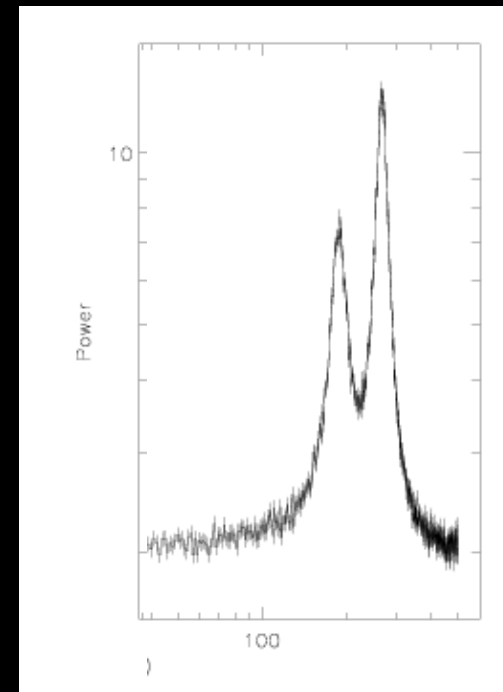
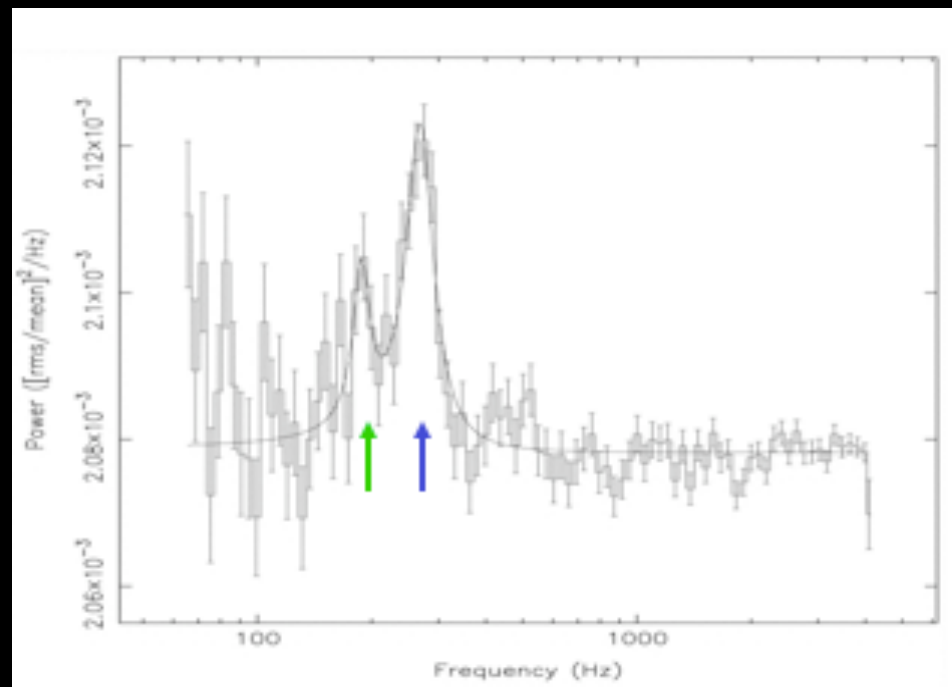


(Fragile & Blaes 2008)

Example: high frequency QPOs in the BHC XTE J1550-564

$v_1 = 188$ Hz, $v_2 = 268$ Hz, frac rms $v_1 = 2.8\%$,
frac rms $v_2 = 6.2\%$ (Miller et al. 2001),
flux = 1 Crab, RXTE Exposure 54 ks,
significance $\sim 3\text{-}4\sigma$

LOFT simulation: $T_{\text{exp}} = 1$ ks

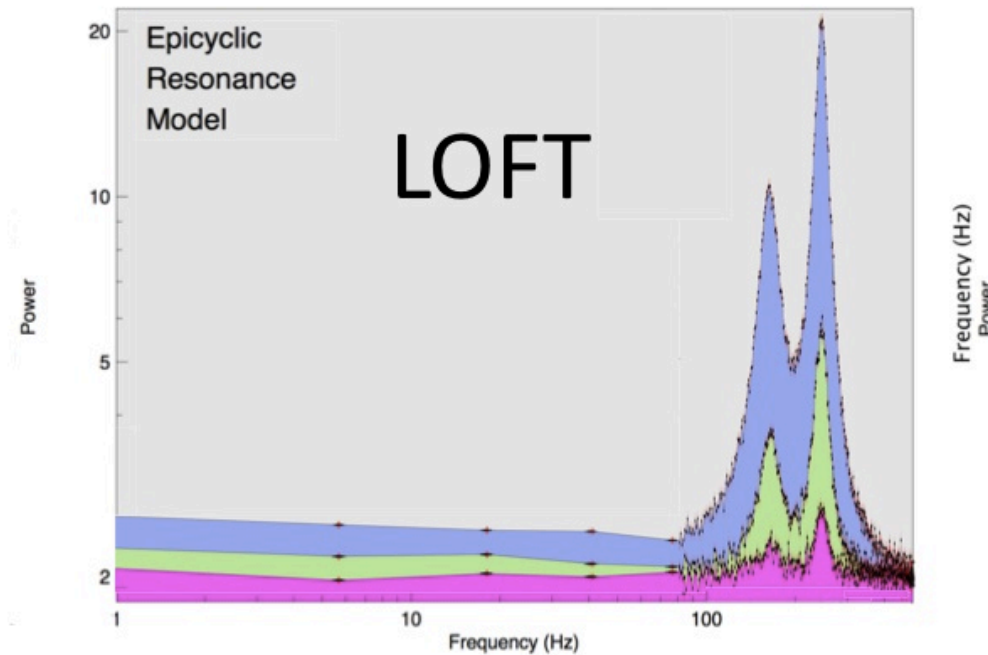


LOFT study of the QPO evolution with flux

Epicyclic Resonance Model

(Abramowicz & Kluzniak 2001)

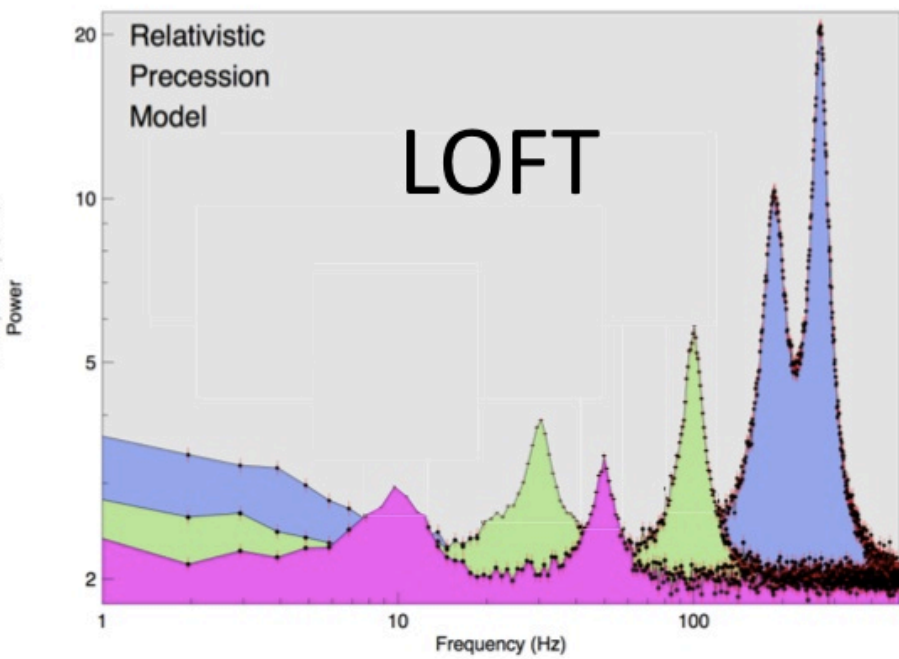
Predicts fixed frequencies



Relativistic Precession Model

(Stella et al 1999)

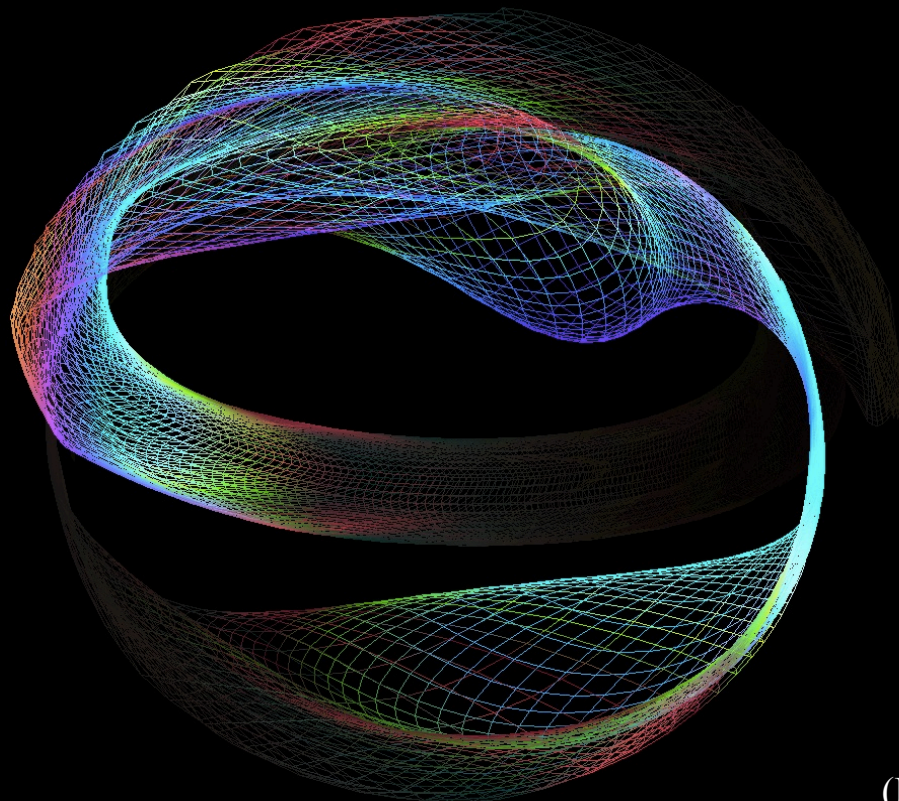
Predicts variable frequencies



Once the ambiguity of the interpretation of the QPO phenomena is resolved, the frequency of the QPOs will provide access to general relativistic effects (e.g. Lense-Thirring or strong-field periastron precession) and to the mass and spin of the black hole.

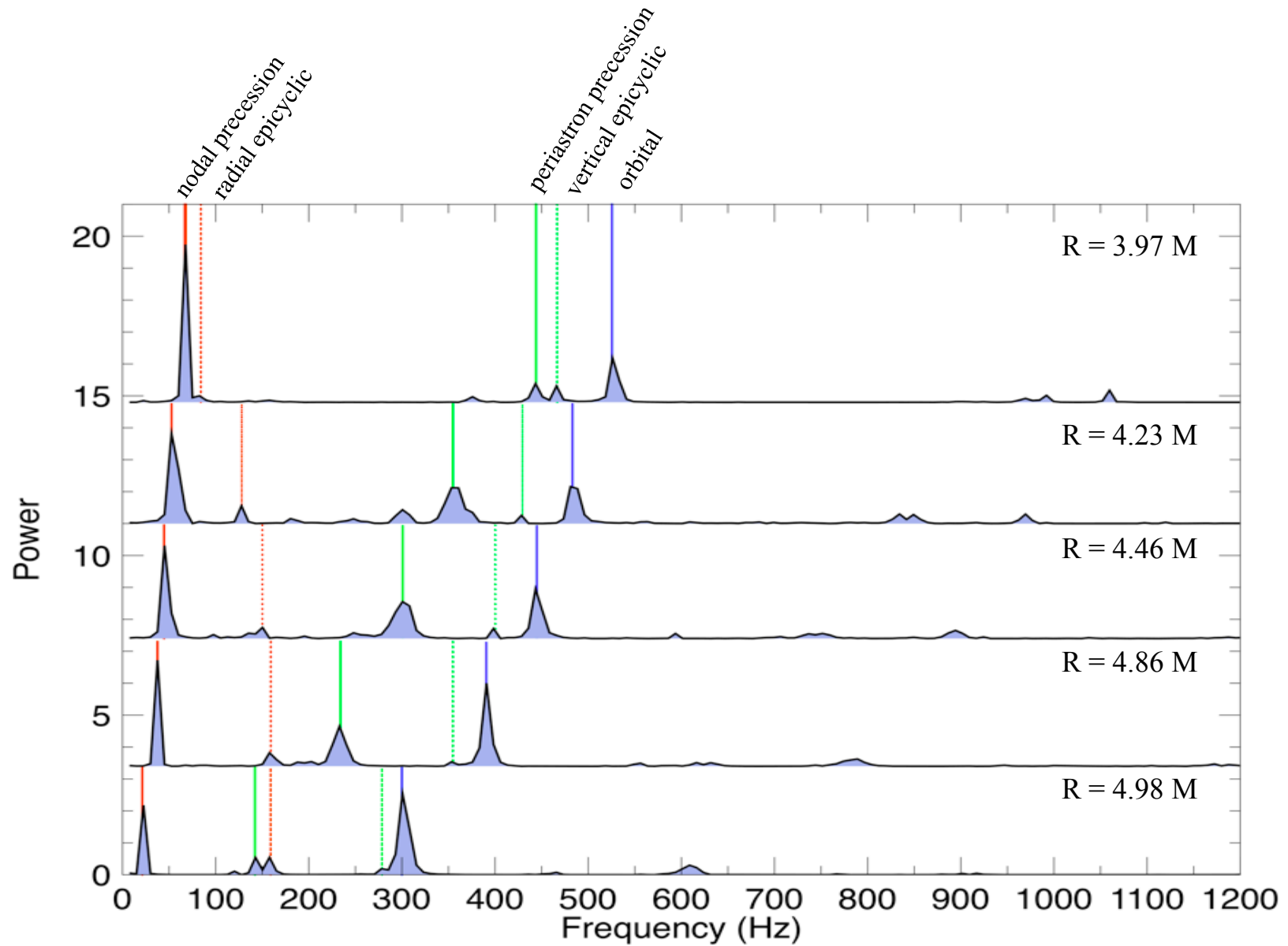
Blob orbiting a Kerr black hole

- Azimuthally-elongated, tilted and eccentric blob to reproduce observed power spectra (GRO J1655–40) within relativistic precession interpretation
- $M = 7.1 M_{\odot}$, $a/M = 0.6$, $I = 63$ deg, variable $R \sim 4-5 M$



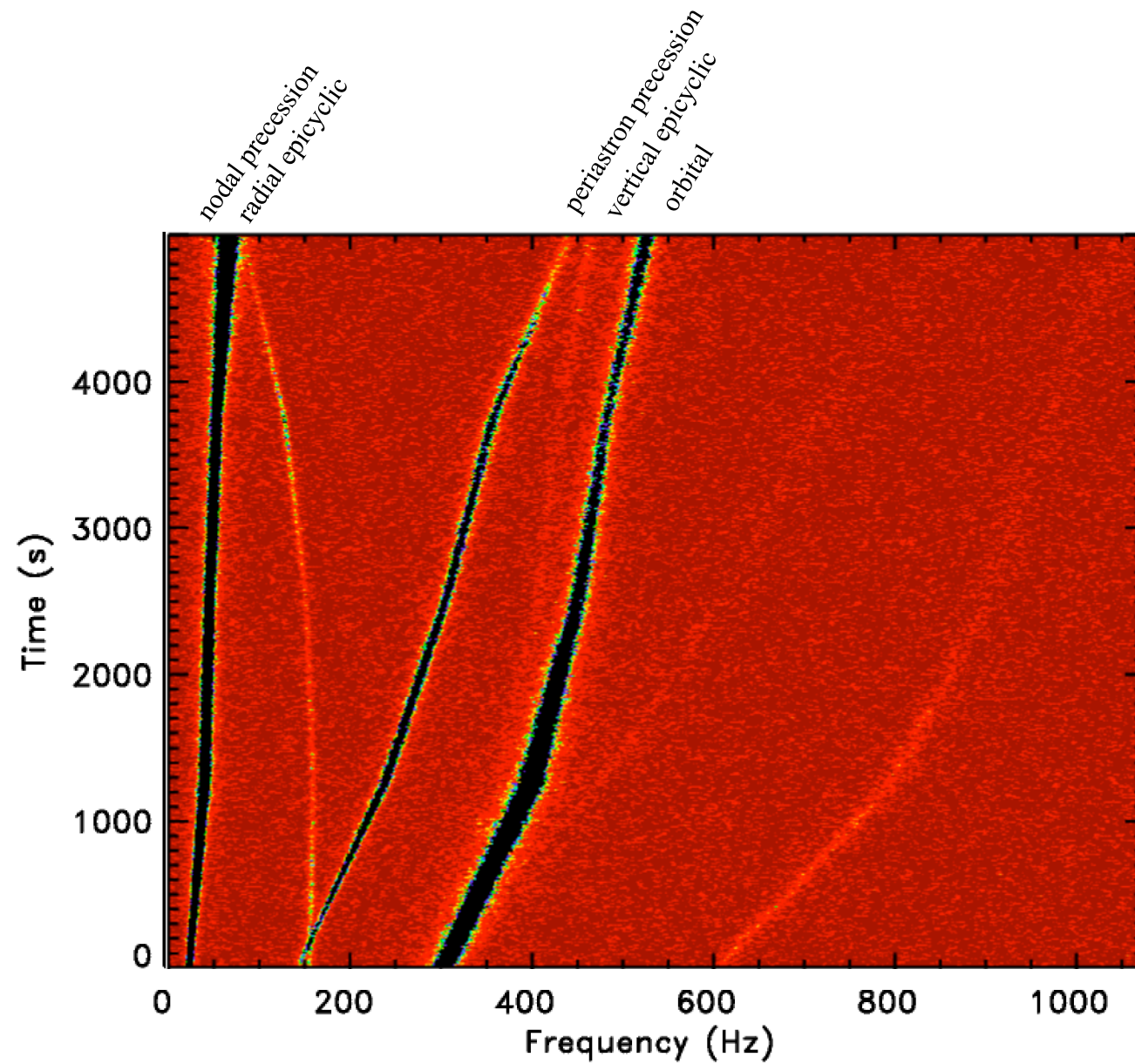
(Bakala, Goluchová, Torok)

Power spectrum for varying emission radii



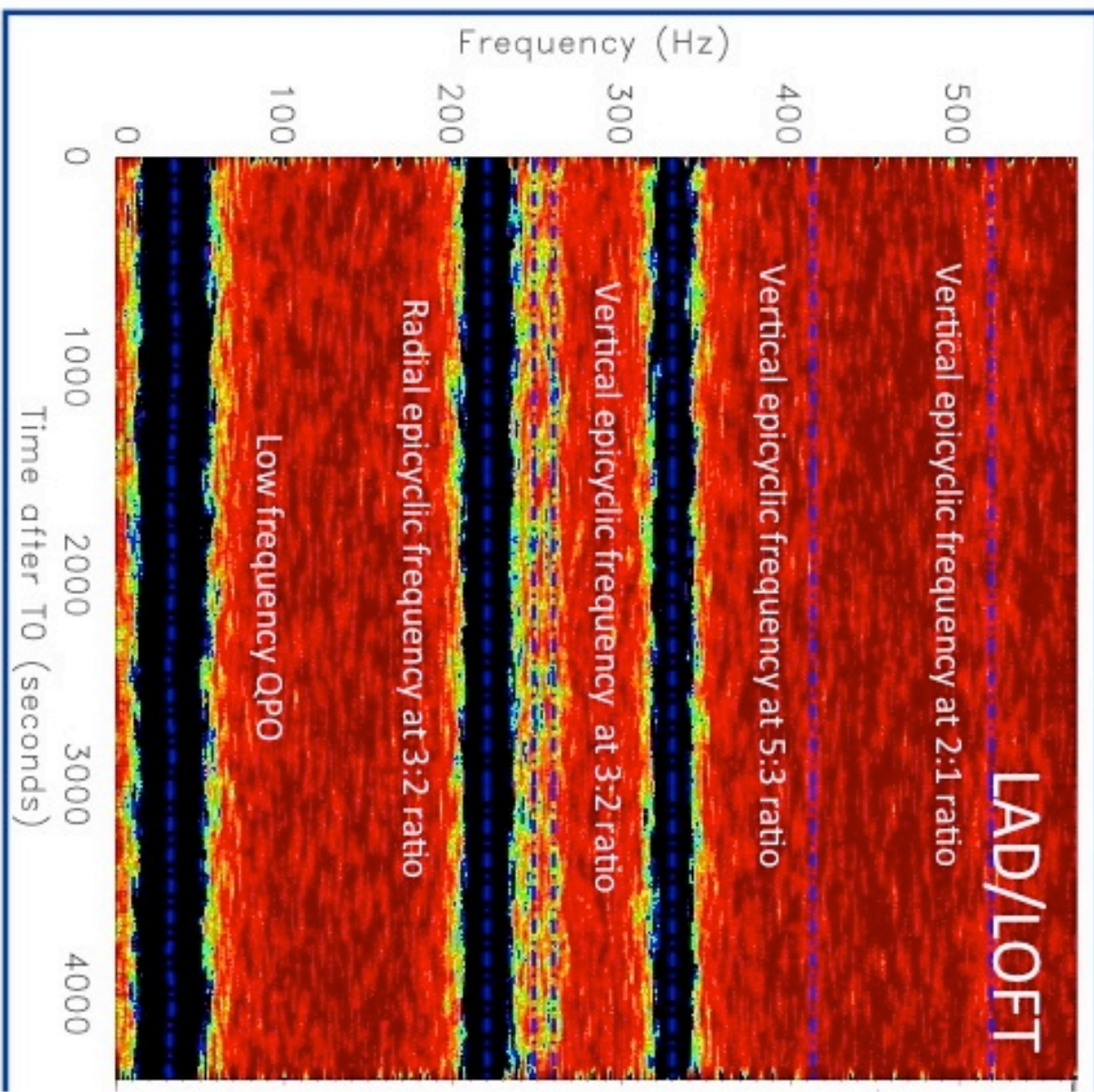
(Bakala, Goluchová, Torok)

LOFT simulation



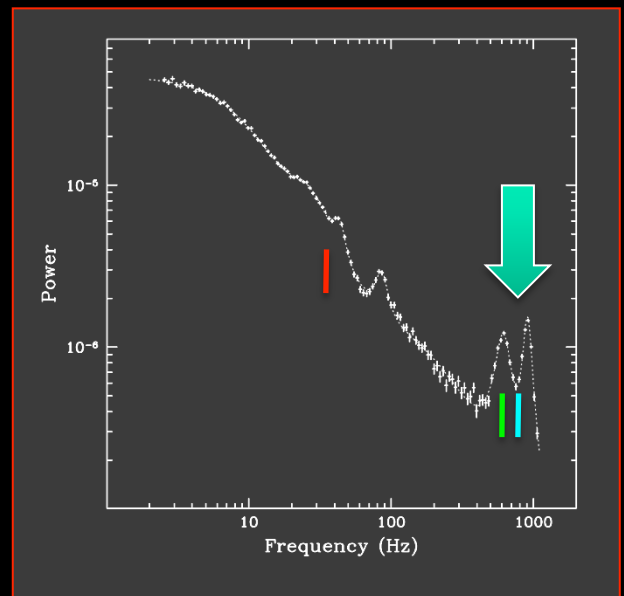
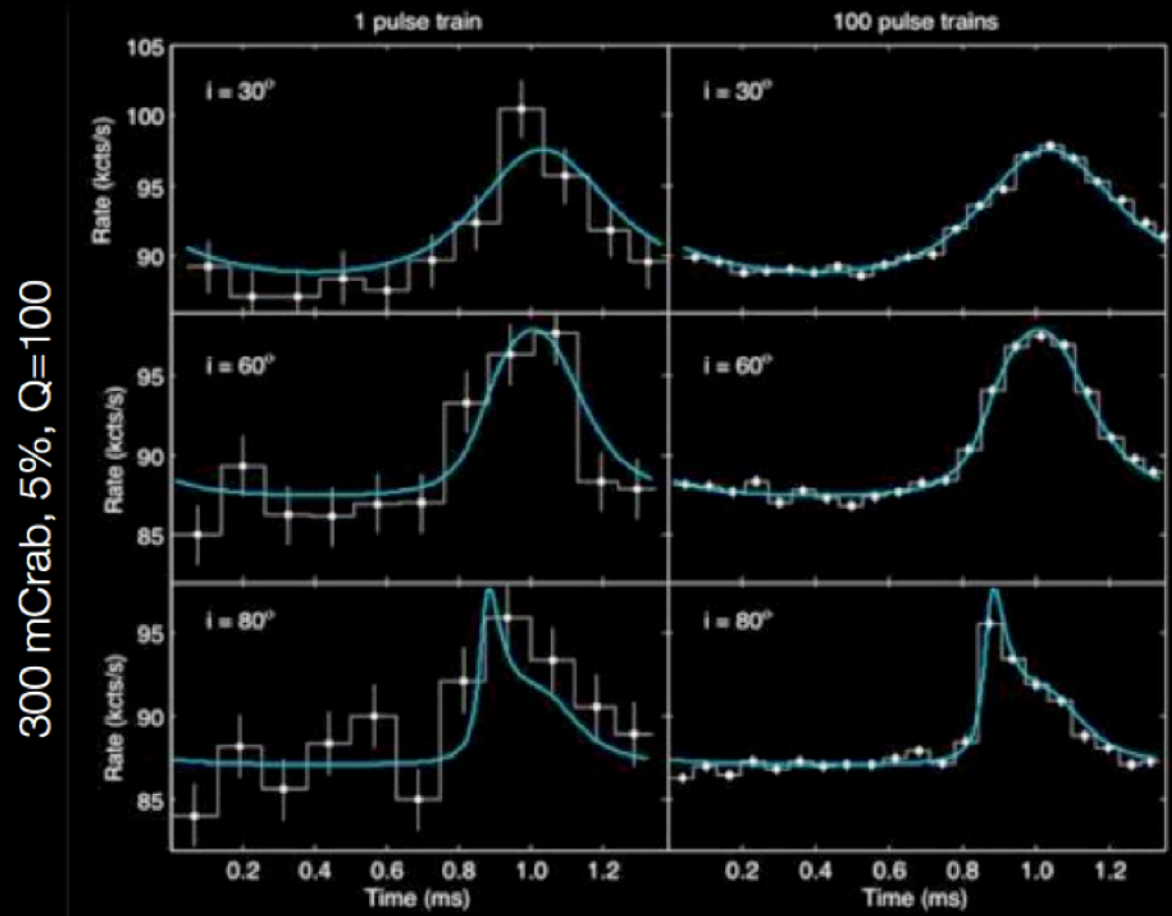
(Barret)

Relativistic Epicyclic Resonance Interpretation



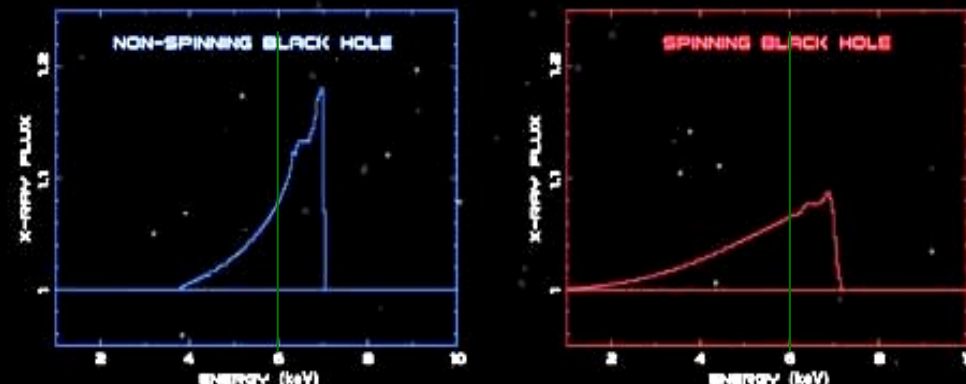
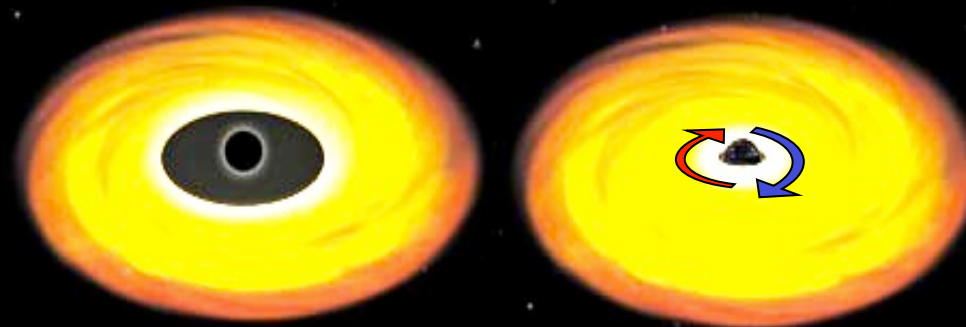
(Barret)

kHz QPOs in Time Domain with LOFT



Strong Gravity diagnostic Fe-lines from accretion disks

- Strong field relativistic effect:
Doppler shifts and boosting,
gravitational redshift, strong field
lensing
- Observed in many Active Galactic
Nuclei and X-ray binaries

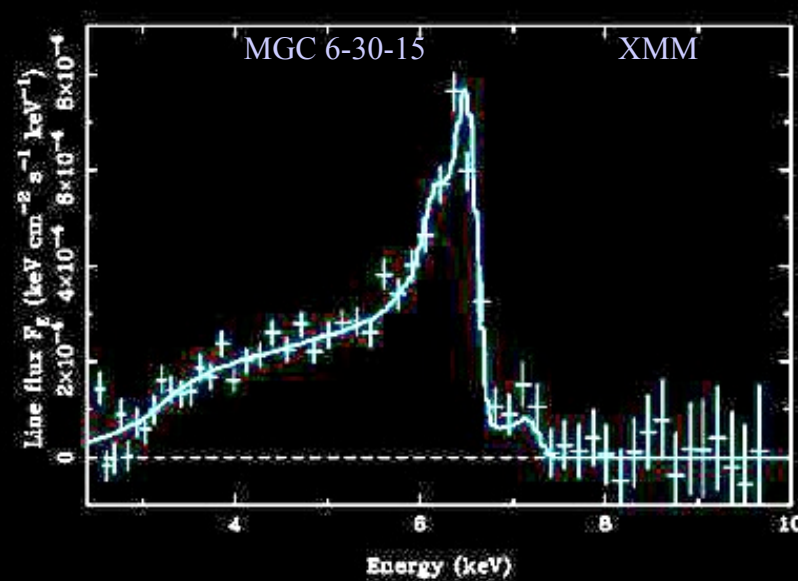


Line profile and time variability
black hole mass and spin

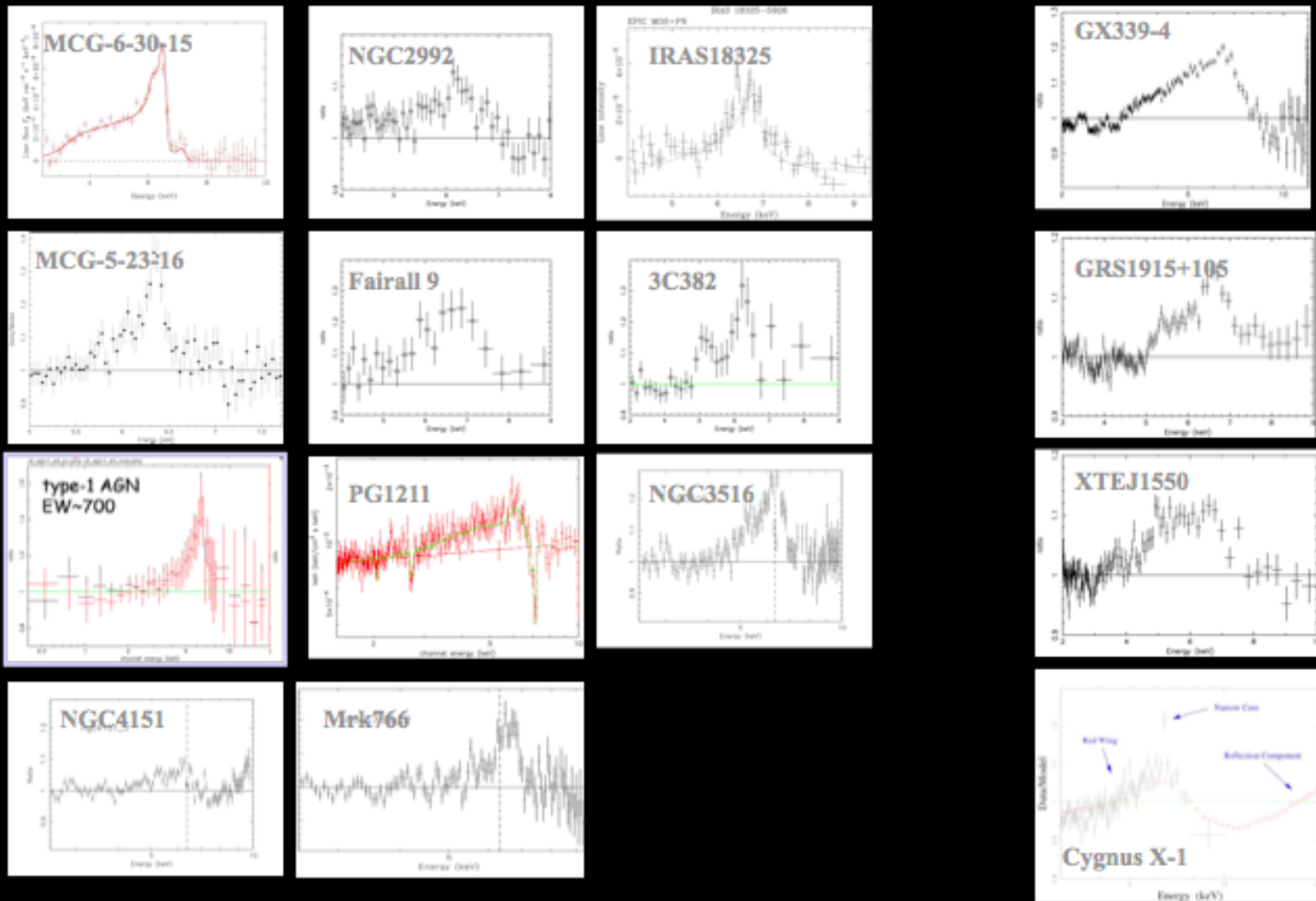
In situ probing of strong field gravity
(~few R_s)

e.g. MCG 6-30-15:

- Kerr BH required to fit line profile



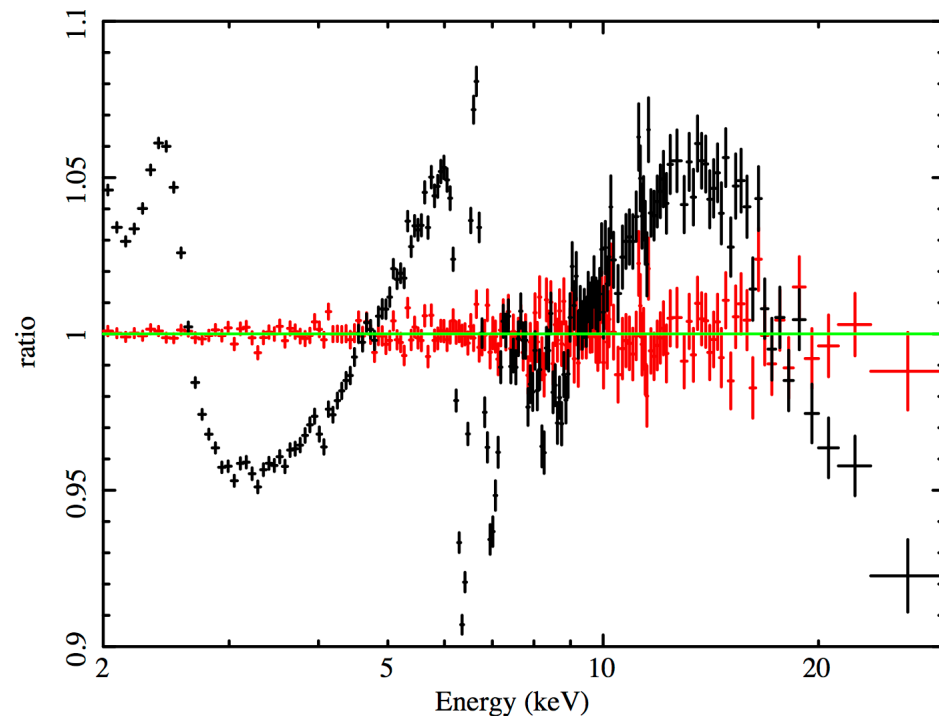
Very Broad Fe-K line profiles in: AGNs X-ray Binaries



Reflection vs complex absorption:

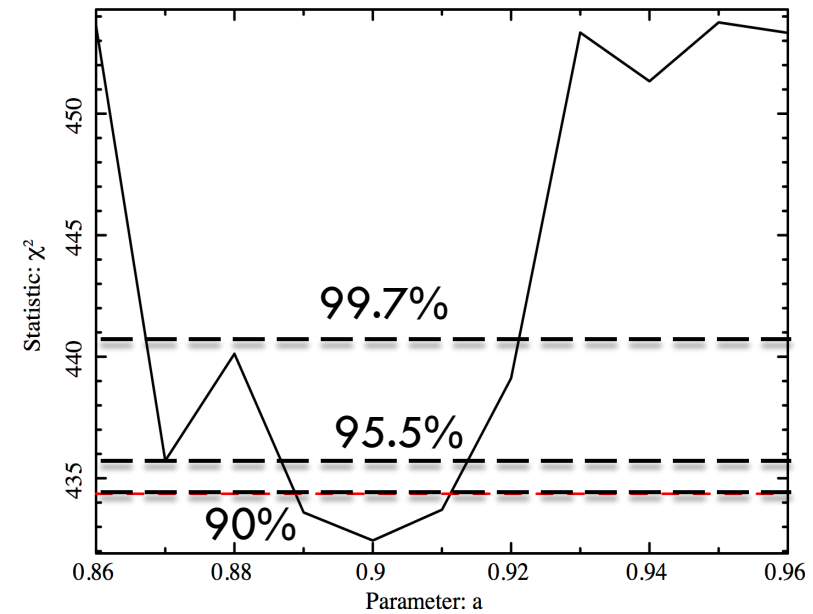
MCG-6-30-15

150 ks LOFT simulated observation



Reflection + blurred Fe line

Complex absorption + distant reflection



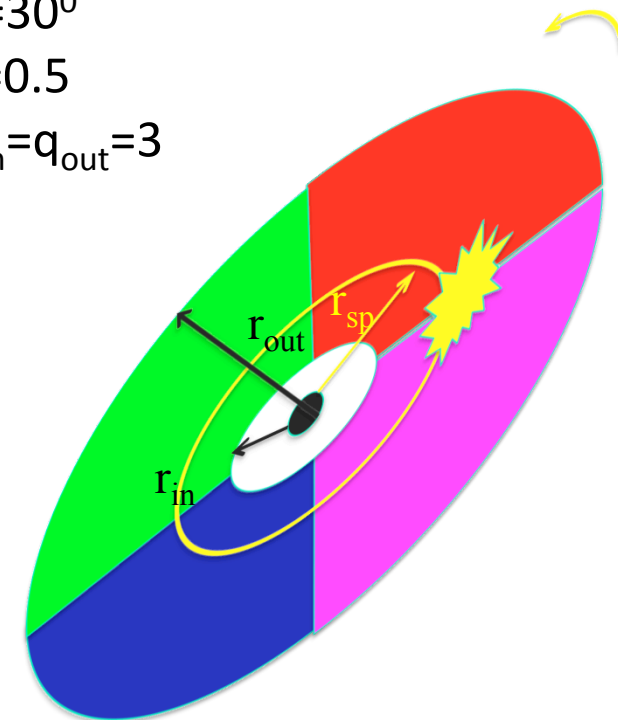
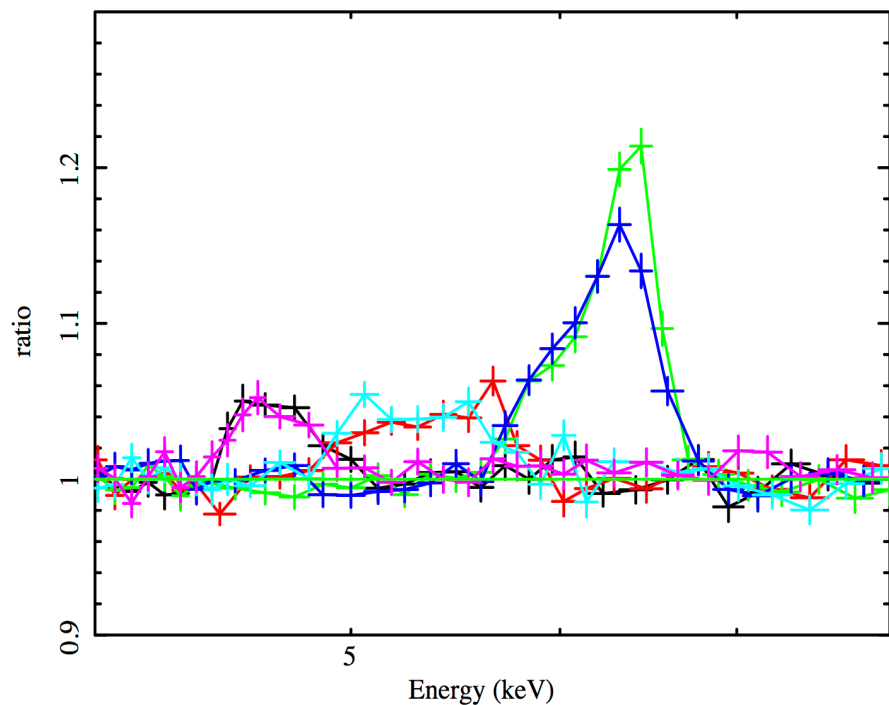
courtesy De Rosa

Tomography: AGN: $3 \times 10^7 M_\odot$, 1mCrab, $a=0.5$, hot spot at $r=r_{\text{isco}}$, variable Fe-line

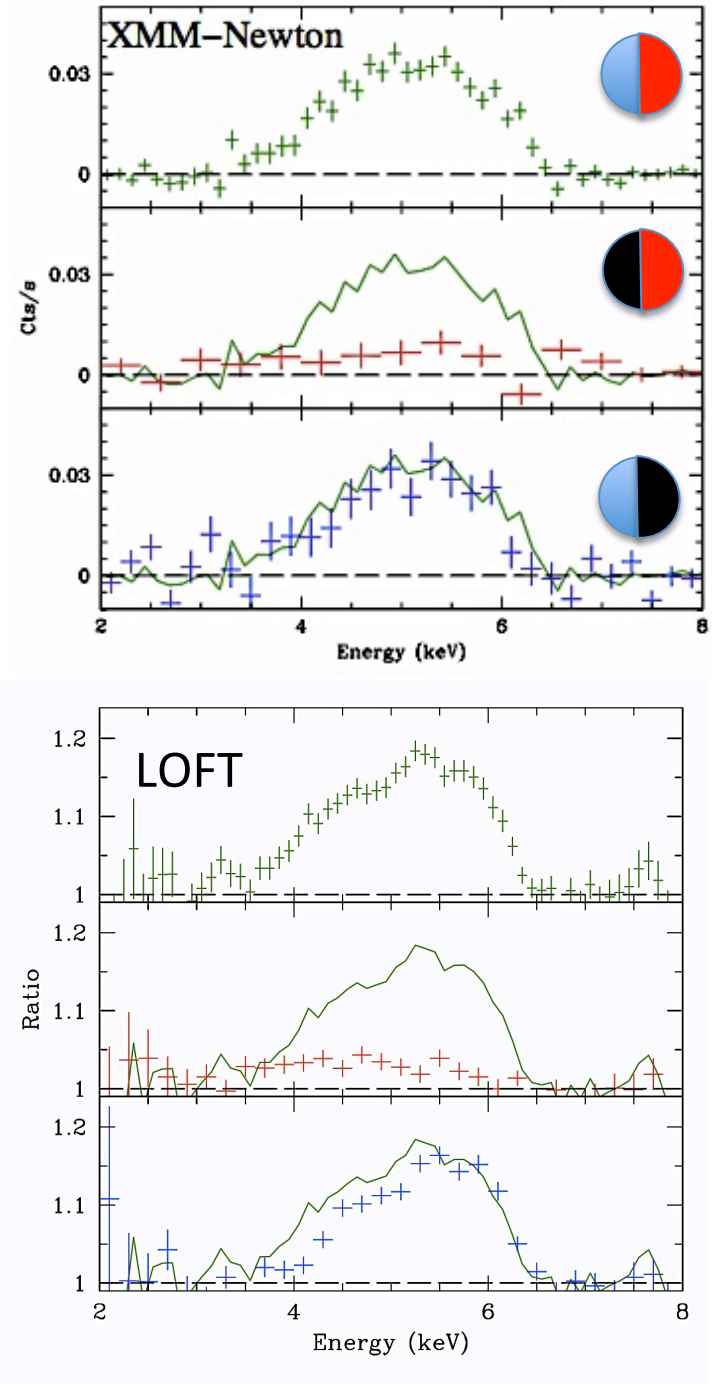


Courtesy De Rosa

- 2 orbits
- 10 phases: 5×10^3 s each
- $R_{\text{sp}} = R_{\text{isco}}$
- $\theta = 30^\circ$
- $a = 0.5$
- $q_{\text{in}} = q_{\text{out}} = 3$



(see Simon Vaughan's talk)



2. Probing SG effects with x-ray “eclipses”

Credits of G. Risaliti

An obscuring cloud covers/uncovers different parts of the accretion disc at different times, allowing a direct check of the expected pattern of disc emission

$$E=6.68+0.03 \text{ keV}$$

$$\text{EW}=340+35 \text{ eV}$$

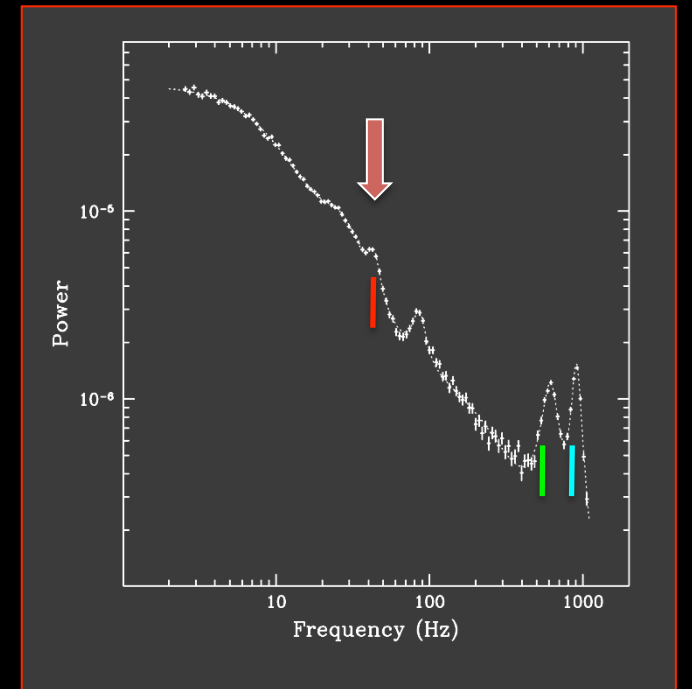
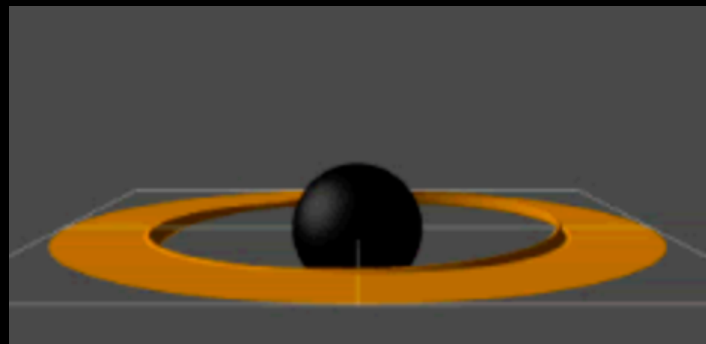
$$R_{\text{in}}/R_{\text{out}}=2.7/400 R_g$$

$$\text{NH}=1\text{e}25 \text{ cm}^{-2}$$

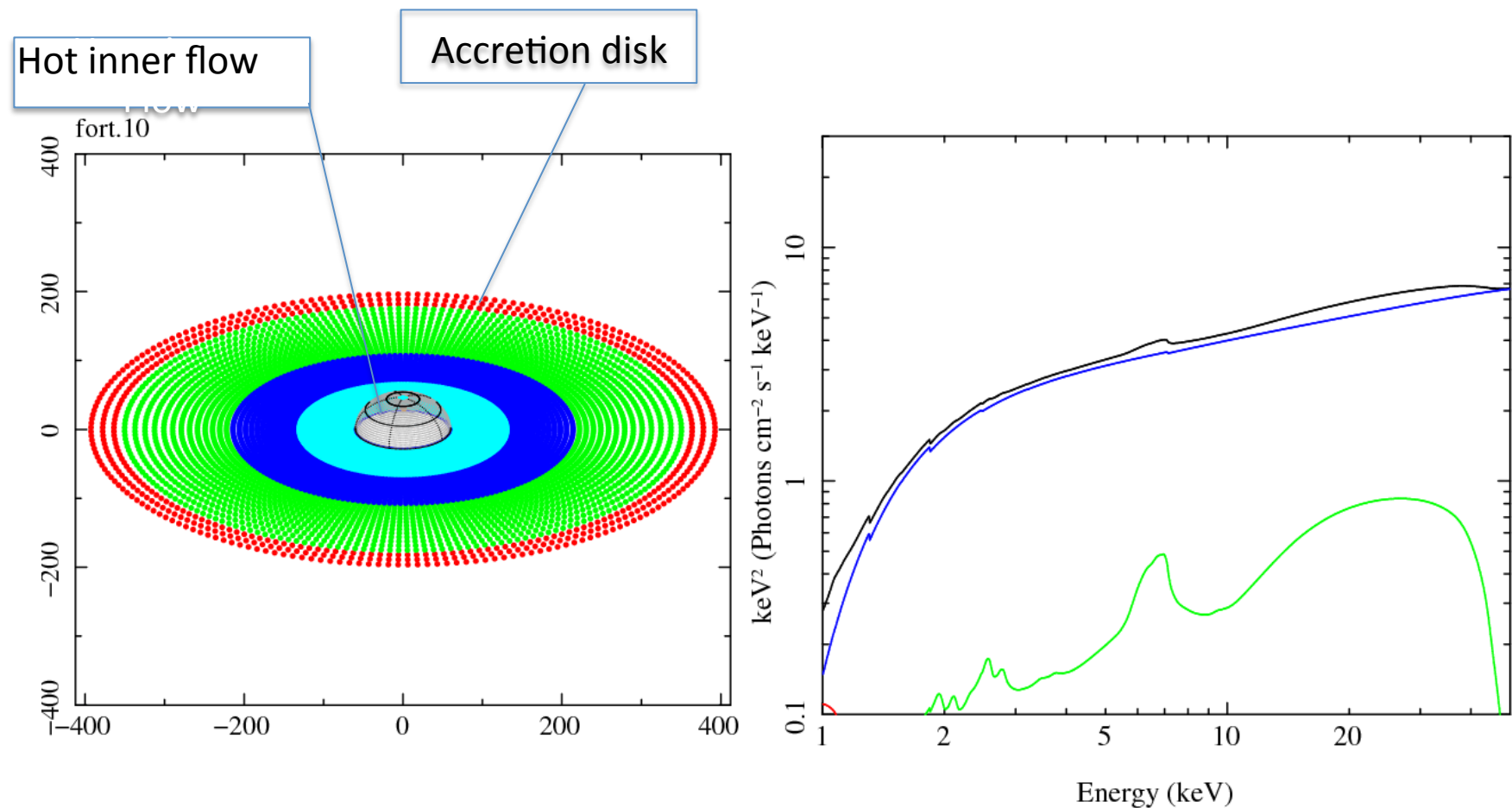
$$T=25\text{ks}+25\text{ks}$$

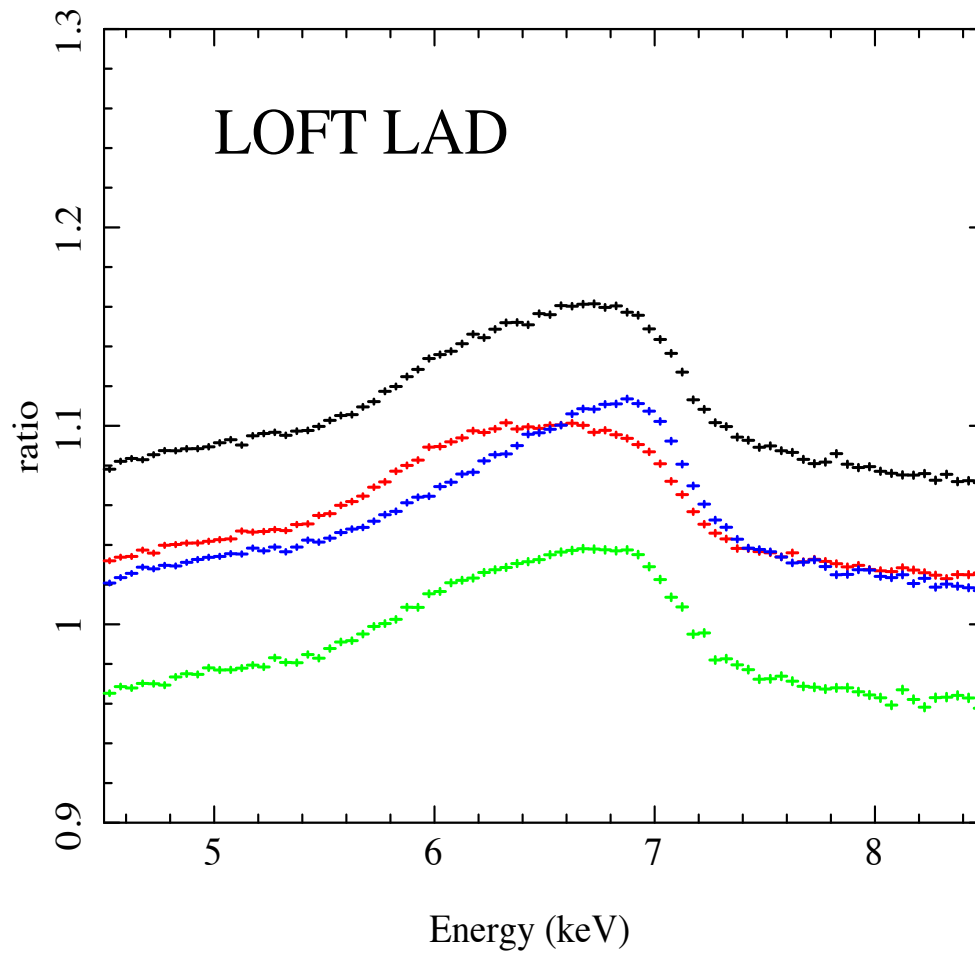
Low Frequency QPOs

Relativistic nodal precession
(from frame dragging)
of the innermost disk regions ?



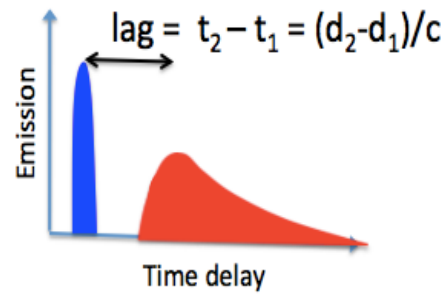
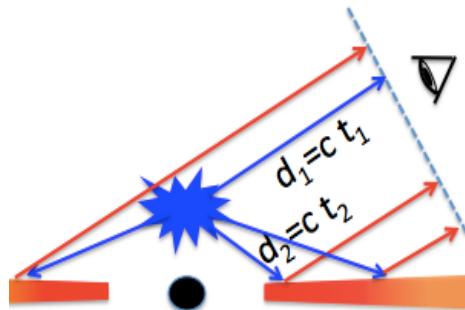
Relativistic nodal precession (from frame dragging) of the innermost disk regions
(Ingram & Done 2012)



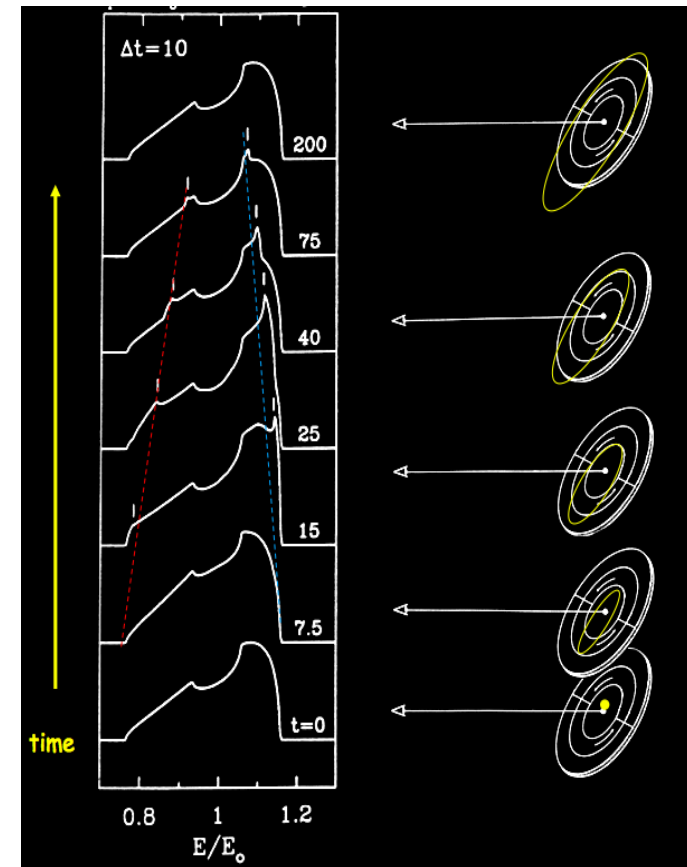


(see Adam Ingram's talk)

Reverberation



in the continuum

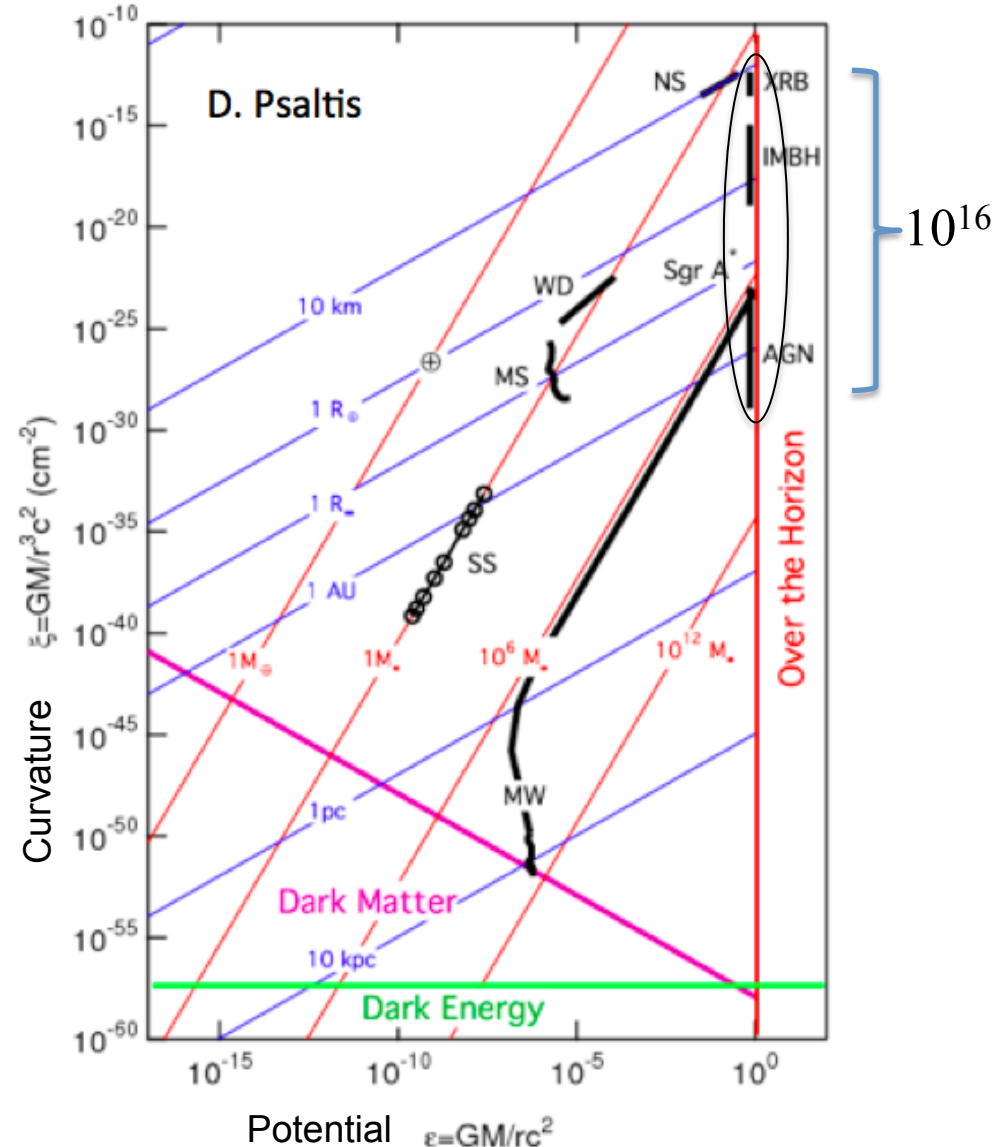


in the Fe-line

(see Phil Uttley's talk)

Black hole no-hair theorem

- GR predicts that motion of matter is determined by M and a ; space time curvature is irrelevant
- LOFT will study in detail the same phenomena (Fe-lines and QPOs) over a factor of 10^8 in mass, or a factor of 10^{16} in space-time curvature
- > Constrain further any violation of the “no-hair theorem”



Yellow Book Strong Gravity Section

2.3 Strong Gravity	3
2.3.1 Overview	3
2.3.1.1 Context	3
2.3.1.2 Basic diagnostics & interpretation.....	6
2.3.1.3 Models and simulations	8
2.3.1.4 Strong Field Gravity with LOFT.....	9
2.3.2 Relativistic line profile variability as probe of strong field gravity	11
2.3.2.1 Precessing inner hot flow	11
2.3.2.2 Reverberation	12
2.3.2.3 Orbiting blob Doppler tomography.....	13
2.3.2.4 Eclipse mapping	15
2.3.2.5 Average line profiles	15
2.3.5 High frequency QPOs as a probe of strong field gravity	16
2.3.5.1 Epicyclic motion in black hole high frequency QPOs	16
2.3.5.2 Relativistic waveform distortions in neutron star kiloHertz QPOs	17
2.3.5.3 Average power spectra	18